



Characterization and evaluation of tea bag papers

Durgesh K. Jha¹ · Pallavee P. Dhekne¹ · Ashwin W. Patwardhan¹

Revised: 25 February 2020 / Accepted: 11 March 2020 / Published online: 16 March 2020
© Association of Food Scientists & Technologists (India) 2020

Abstract The infusion kinetics of tea bags containing black tea or green tea has been studied in detail in the past. However, the tea bag papers have never been characterized and evaluated earlier to understand their contribution towards tea bag infusion. In the present work, papers used for making tea bags were characterized for thickness, wettability, surface topography, pore size, porosity and permeance to understand their influence on infusion kinetics of tea bags. Scanning electron microscopy studies highlighted the pore structure and porous nature of tea bag papers. The porosity of tea bag paper was quantified using image processing and permeance was determined experimentally. Besides, a relationship between porosity and permeance of tea bag papers has been perceived. A general trend of increase in permeance with increasing porosity was observed. Woven nylon paper showed the highest permeance (23.9×10^{-5} m/s) when compared with other tea bag papers. Furthermore, an initial infusion rate was determined using initial infusion data of tea bag infusion for different tea bag papers. The influence of permeance on the initial infusion rate of tea bag papers has also been investigated.

Keywords Tea bag papers · Contact angle · Permeability · Permeance · Porosity · Infusion rate

List of symbols

\overline{P}_M Permeance (m/s)
 \overline{A} Average pore area (m²)

A Area of the tea bag paper (m²)
a Cross-sectional area of the sample (m²)
 C'_1 Concentrations of solute at feed and paper interface (kg/m³)
 C'_2 Concentrations of solute at paper and permeate interface (kg/m³)
 C_0 Concentration of solute (kg/m³) at time $t = 0$
 C_1 Feed phase concentration of the diffusing solute (kg/m³)
 C_2 Permeate phase concentration of solute (kg/m³)
 D_M Tea bag diffusivity (m²/s)
D Average pore size
F Force (N)
g Gravitational constant (m/s²)
h Immersion depth (m)
P Wetted perimeter of the sample (m)
 k_1 Mass transfer coefficient in feed liquid phase (m/s)
 k_2 Mass transfer coefficient in permeate liquid phase (m/s)
 l_M Thickness of TB paper (m)
 N_A Flux of solute gallic acid (kg/m² s)
V Volume of feed and permeate (m³)

Greek symbols

θ Contact angle (°)
 γ Surface tension (N/m)
 ρ Density of fluid (kg/m³)

Introduction

Consumers across the globe follow various brewing habits for tea preparation. Loose tea and tea bag brewing are the two most commonly used methods. However, tea bags are becoming popular for tea brewing across the world because

✉ Ashwin W. Patwardhan
aw.patwardhan@ictmumbai.edu.in

¹ Department of Chemical Engineering, Institute of Chemical Technology, Matunga, Mumbai 400019, India

of its convenience and simplicity. As per the UK Tea & Infusions Association, around 96% of the British market is covered by tea bags (UK Tea & Infusions Association 2010). The common practice of brewing tea in India is to boil the loose tea leaves or tea particles.

The factors affecting the infusion rate of tea solutes have been widely studied in the past (Price and Spiro 1985; Spiro et al. 1992; Price and Spitzer 1993; Jaganyi and Mdletshe 2000; Astill et al. 2001; Jaganyi and Ndlovu 2001; Suteerapataranon et al. 2009; Joshi et al. 2016; Farakte et al. 2016; Yadav et al. 2017). Price and Spiro (1985) studied the black tea leaf and investigated the effect of leaf size and manufacturing method on the infusion kinetics of caffeine and theaflavins. They showed that the rate constants increased with decreased leaf size. Spiro et al. (1992) compared the caffeine extraction rates from large leaf black and green teas and found that the caffeine diffusion through the leaf was a greatly hindered process. Their results also suggested that smaller leaf size offers lower hindrance to diffusion process. Farakte et al. (2016) reported that the rate of infusion was found to be higher for small particle sizes and higher temperature. Jaganyi and Mdletshe (2000) studied the hindrance effect of tea bag material on the infusion rate of caffeine at various temperatures. Their results suggested that the tea bag material slowed the caffeine infusion rate over the temperature range as suggested by the first order rate constant which was found to be 29% lesser as compared to that of loose tea. The lesser first order rate constant is a consequence of resistance offered by tea bag material. Astill et al. (2001) studied the influence of tea bag design (i.e. shape and size) and the brewing method (i.e. dynamic and static infusion) on the final infusion compositions. The flow resistance offered by the bed of tea granules and the bag material results in the slower infusion rate irrespective of bag design or brewing method. Jaganyi and Ndlovu (2001) studied the rate of caffeine infusion as a function of tea bag size and shape. The infusion rate constant varied with tea bag size but found to be independent on shape. Yadav et al. (2017) investigated the infusion rate as a function of the bag dipping rate, tea particle size, tea granules loading and tea bag shapes. The infusion rate of tea bag decreased with increased tea granules loading in tea bags. Dhekne and Patwardhan (2020) developed the tea bag infusion model which also suggests that packed bed of tea granules significantly affects the swelling rate and consequently infusion rate.

Most of the research to date has been dealt with the effect of tea bags on infusion kinetics of tea. Although most of the teas across the world are brewed using tea bags, information regarding the impact of tea bag paper parameters on tea bag infusion is slender. Thus, there is a great need for the characterization of tea bag paper parameters, which will eventually influence infusion kinetics of tea bags. The present work reports, for the first time, a detailed

study of the characterization and evaluation of different tea bag paper parameters. The effect of the tea bag parameters on their infusion kinetics has also been investigated. The contribution of pore size and fiber network on porosity is also discussed.

Materials and methods

Crush, Tear, Curl (CTC) black tea was purchased from the local market. De-ionized (DI) water (Millipore Inc, USA) was used throughout the experiments and analysis. Cellulosic tea bag papers were provided by Sikri Packaging Corporation LLP, Kolkata, India. Polylactic acid (PLA) and nylon tea bag papers were purchased from Kaiquinmomo store, China. Double chambered (DC) tea bags (6.5 cm × 4 cm) were made in-house using these papers.

Attenuated total reflectance Fourier transform infrared (ATR-FTIR) spectroscopy

ATR-FTIR spectroscopy generates the infrared vibrational spectrum, interpretation of which, allows identification of functional groups of the material. Fourier Transform Infrared (FTIR) spectra of Cellulose, Cellulose/Polypropylene, Polylactic acid (PLA) and nylon tea bag papers were collected in the region from 400 to 4000 cm^{-1} with a resolution of 4 cm^{-1} , after appropriate background subtraction, using FTIR-4600 type A equipped with ATR PRO ONE accessory (Jasco, Japan). Attenuated Total Reflectance (ATR) FTIR was used to record the spectrum, which enables a direct measurement of the sample. The number of scans per spectrum was 32.

Thermogravimetric analysis (TGA)

TGA is a thermal technique wherein the sample is heated and loss in the weight is recorded as a function of time and temperature. The loss in the weight of the sample could be because of chemical or physical changes during heating. The thermal stability of the tea bag papers was carried out with DTG-60H simultaneous DTA-TG apparatus (Shimadzu, Japan). 2–3 mg of samples were added to the alumina crucibles with an empty crucible as a reference. The conditions used to record the thermogram are heating range from 10 to 500 °C at a scanning rate of 20 °C min^{-1} under a nitrogen flow rate of 100 ml/min.

Thickness and grammage measurement

The thickness of the tea bag papers was measured using a micrometre screw gauge (Type E02 Baker, Mercer). Thickness was measured at five different points in a tea bag

paper sample. The average thickness values were calculated and reported along with the standard deviation. Grammage or paper density (g/m^2) of tea bag papers were measured in triplicates using a weighing balance (AUW220D, Shimadzu). Tea bag paper of one square centimeter was cut and weighed.

Contact angle measurement (tea bag wettability)

Contact angle measurement of all tea bag papers was carried out using Kruss Tensiometer (K-100, Germany), which determines the contact angle using a Wilhelmy plate method. In this method, a thin, smooth, vertical paper is brought in contact with a liquid of known surface tension and density. The apparent change in its weight is detected by a balance which is the measure of the force required to immerse in and withdraw the paper from that liquid. The change in force detected on balance is a combination of buoyancy and the force of wetting (Yuan and Lee 2013). The wetting force is the function of contact angle (θ), surface tension (γ) and wetted perimeter (P). The force required to immerse the paper in a liquid can be written as Eq. (1):

$$F = P\gamma \cos \theta - \rho ahg \quad (1)$$

Equation (1) can be solved by linear regression to determine $\cos \theta$. The immersion and withdrawal of the plate correspond to the advancing and receding curve of the measured force versus immersion depth plot, which yields the advancing and receding contact angle, respectively (Son and Gardner 2007).

A tea bag paper of known dimension (5 mm \times 20 mm) was cut and attached to the sample holder vertically. The sample holder was suspended from the balance. The dimension of the paper was optimized to the known dimension after studying the contact angle of tea bag papers ranging from large to small sizes. The sample paper was allowed to dip up to 5 mm into the distilled water at an immersion speed of 3 mm/min. As sample contacted with the water surface, the water rose up due to capillary action. The sample was immersed further in water and the increase of buoyancy caused a decrease in the force detected on balance. This force was automatically recorded and used for the calculation of advancing contact angle.

Similarly, the force was measured for the receding contact angle when the paper was withdrawn from water. The analysis was performed in triplicate on three different samples of the same dimensions. The average value was reported along with the standard deviation.

Scanning electron microscope (SEM)

The surface topography and average pore size of tea bag papers were determined using a scanning electron microscope (JSM-5200, Jeol, Japan) operating at an accelerating voltage of 15 kV. A small section of tea bag paper was placed on aluminum stubs using double-sided adhesive carbon tape and coated with platinum for 20 s using a platinum sputter coater (Polaron Model SC7640). Tea bag paper images at various magnifications were taken using the software.

Pore area, pore size, and porosity measurement

Pore area, pore size and porosity measurements were performed on SEM images of tea bag papers using image analysis software (ImageJ2x). The scale given on the SEM image was used for the calibration of pixel to μm . The SEM image of tea bag papers was then processed in ImageJ2x. During processing, the threshold of the SEM image was adjusted and then converted into a binary image.

The voids present between three or more fibers were considered as pores. Thus, such voids present in the tea bag paper were identified as pores and the software measured the pore area. More than 500 pores were analyzed for each tea bag paper. The whole range of pore area was divided into various bins of size $500 \mu\text{m}^2$. The number of pores in the respective bin size (frequency, n_i) was calculated. Using the frequency (n_i), the % frequency for a particular bin was calculated with respect to the total pore area. Then, the % frequency was plotted against the pore area range to get pore area distribution for each tea bag paper. The average weighted mean pore area was calculated using Eq. (2).

$$\bar{A} = \frac{\sum_{i=1}^N A_i \times n_i}{\sum_{i=1}^N n_i} \quad (2)$$

where A_i denotes the average bin area.

The pores present in the tea bag papers were random and of different shapes and sizes. Therefore, for the sake of the average pore size calculation, pore shape was assumed to be square. Thus, the average pore size was calculated as $D = \sqrt{\bar{A}}$. The total area of the SEM image of tea bag paper under investigation was measured using the software. The summation of all the void areas present within the defined area gave the total pore area (μm^2) of that tea bag paper. The ratio of total pore area to the total area of the SEM image determined the porosity (void fraction) of the investigated tea bag paper. The percent porosity of each tea bag paper was determined and reported throughout the study.

Permeability study

Permeability of a tea bag paper depends on the pore size and porosity of the bag. To determine the permeability of the tea bag paper, experiments were performed and the data were fitted into the permeability model.

Permeability experiment

For determining the permeance of tea solutes through various tea bag papers, concentrated tea brew from tea infusion was used. Concentrated tea brew was prepared using 2 g of tea infused in 30 ml of DI water at 60 °C at 300 ± 10 rpm for 15 min in a vessel. After 15 min, the experiment was stopped and the brew was filtered immediately. The total volume of the filtrate obtained was measured. Of this, 20 ml of concentrated brew was used as a feed phase in permeability experiments.

Mass transport of tea solutes across the tea bag paper from the feed phase (tea brew) was studied using a two-compartment permeation cell. The experimental set-up used for measuring the permeability of the tea bag paper is shown in Fig. 1a. A tea bag paper was cut into a circular disc of an area of $9.621 \times 10^{-4} \text{ m}^2$ and placed in the membrane acrylic holder. Permeability experiment was performed at room temperature. Feed and permeate cells were filled with 70 ml of DI water each. 20 ml of concentrated infusion of known concentration and 20 ml DI water was added to 70 ml of DI water in feed and permeate cells, respectively. The feed and permeate phases were mechanically stirred at 100 rpm to avoid concentration polarization at the tea bag paper interfaces. The stirring speed of mechanical stirrer as 100 rpm was decided after optimization over 40–100 rpm for performing the permeability experiments. During the experiments, 0.3 ml samples were withdrawn from feed and permeate phases each

for the determination of Gallic acid equivalent (GAE) concentration. The samples were suitably diluted and absorbance was measured at 272 nm using UV–Visible Spectroscopy (Cary varian 50) (Farakte et al. 2016). The majority of the tea polyphenols and catechins are Gallic acid (GA) derivatives (Harbowy and Balentine 1997). Hence, the absorbance measured at 272 nm wavelength was determined as Gallic acid equivalent (GAE). Permeance was determined by calculating GAE concentrations in the feed phase as a function of time.

Permeation model

The quasi-steady-state concentration profile for solute transport through tea bag paper is depicted in Fig. 1b. The tea solutes are transported from the feed phase to the permeate phase via diffusion through feed side film, pores of the tea bag paper and then into permeate side film.

The film theory can be applied to mass transport of tea solutes through tea bag paper. The rate of solute transport can be expressed as a function of the solute concentrations by writing quasi-steady-state mass flux equations across the tea bag paper. It can be represented using Eqs. (3, 4, and 5).

$$N_A = k_1(C_1 - C'_1) \tag{3}$$

$$= \frac{D_M}{l_M}(C'_1 - C'_2) \tag{4}$$

$$= k_2(C'_2 - C_2) \tag{5}$$

where C_1 is the feed phase concentration of the diffusing solute GA in kg/m^3 and C_2 is permeate phase concentration of solute GA in kg/m^3 . The interface concentrations of solute for the feed and permeate side is denoted by C'_1 and C'_2 respectively. Rearrangement of above Eqs. (3), (4) and (5) in terms of C_1 and C_2 gives,

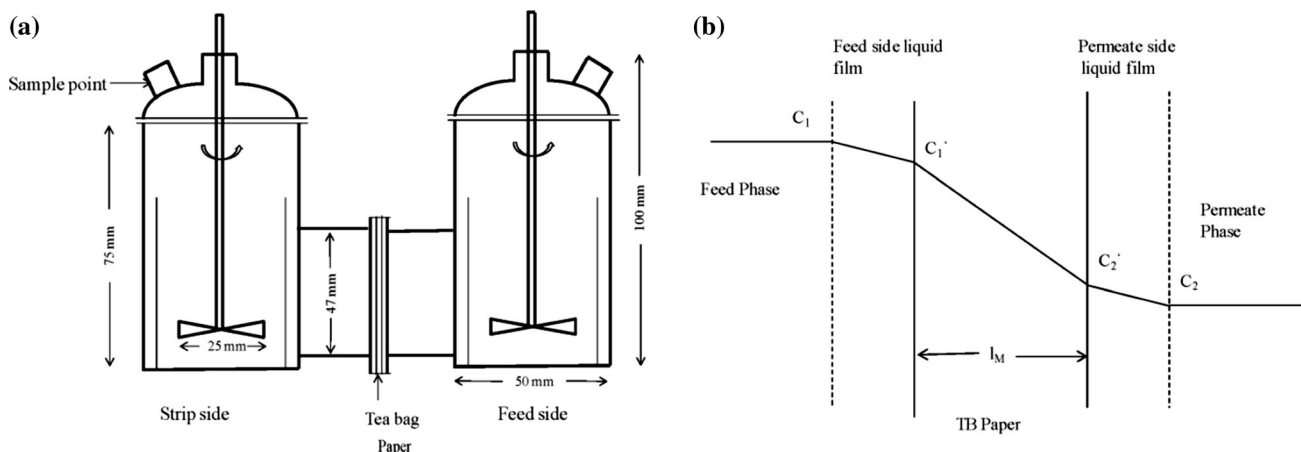


Fig. 1 Schematic representation of **a** two-compartment permeation cell set-up, **b** concentration profile for solute flow through tea bag (TB) paper

$$N_A = \frac{1}{\left(\frac{1}{k_1} + \frac{l_M}{D_M} + \frac{1}{k_2}\right)} (C_1 - C_2) \quad (6)$$

where l_M is the tea bag paper thickness in m, and D_M is tea bag diffusivity in m^2/s . The liquid film mass transfer resistances ($1/k_1$ and $1/k_2$) are quite small compared to the tea bag paper resistance; therefore, the liquid film mass transfer resistances are negligible. Since, the tea bag paper resistance (l_M/D_M) controls the permeation rate, the Eq. (6) can be rewritten as follows,

$$N_A = \bar{P}_M (C_1 - C_2) \quad (7)$$

where, $\bar{P}_M = D_M/l_M$ is the permeance in m/s .

The flux can alternatively be expressed as

$$N_A = \frac{-dC_1}{dt} \left(\frac{V}{A}\right) \quad (8)$$

From Eqs. (7) and (8), we get:

$$\frac{-dC_1}{dt} \left(\frac{V}{A}\right) = \bar{P}_M (C_1 - C_2) \quad (9)$$

where A is the exposed area of tea bag paper, V is the feed volume and C_0 is the initial concentration of tea solutes. For equal volumes, the mass balance of the solute can be written as,

$$C_0 = C_1 + C_2 \quad (10)$$

To determine permeance through tea bag paper, Eq. (9) can be integrated and rewritten as follows:

$$\int \frac{dC}{C_1 - C_2} = \left(\frac{\bar{P}_M A}{V}\right) \int dt \quad (11)$$

At initial conditions: at time $t = 0$, $C_1 = C_0$ and $C_2 = 0$;

$$\ln\left(\frac{C_0}{2C_1 - C_0}\right) = \left(\frac{\bar{P}_M A}{V}\right) t \quad (12)$$

If we plot $\ln(C_0/(2C_1 - C_0))$ against t , the permeance can be determined from the slope of the fitted straight line.

Tea bag infusion study

Tea bag dipping set-up made earlier was used to study the tea infusion kinetics (Yadav et al. 2017). The set-up mimics the vertical dipping of the tea bag in water. The infusion experiments were carried out with a tea bag containing 2 g tea. 100 ml of DI water was poured in a vessel, placed in a water bath and heated to 80 °C. A tea bag was attached to the dipping rod with the help of thread and dipped into the hot water when the desired temperature inside the vessel was achieved. The tea bag was dipped in and out of the water at dipping frequency of 50 dips per minute (dpm). The dipping frequency was optimized

before performing the infusion experiments. 0.5 ml sample was withdrawn at every 10 s interval for the first 3 min and later at 4, 5 and 10 min. Tea bag infusion time was kept as 10 min. After 10 min, the experiment was stopped and the volume of the filtrate was measured. The GAE concentration was determined for the withdrawn samples. The concentration values were corrected for the volume loss caused by evaporation and sampling. The GAE% was calculated for 2 g tea used.

Tea infusion from a tea bag (for the initial 60 s) can be represented by the pseudo-zero order kinetic, as shown in Eq. (13):

$$C_t = k_i t \quad (13)$$

where C_t (mg/ml) is the concentration of tea solutes in infusion at a time 't'; k_i (mg/ml s) is the initial rate for infusion process and t (s) is infusion time. Equation (13) was used for the estimation of the initial rate using tea bag infusion kinetic data. From the plot of C_t versus t , the initial rate can be determined from the slope of the straight line.

Results and discussion

ATR-FTIR spectroscopy

Figure 2 (I) presents the IR spectra of all the tea bag (TB) papers. The characteristic stretching vibrations of cellulosic –OH and –CH were observed in the range of 3660–2900 cm^{-1} (Fig. 2 (I-a), (I-b)). The region of 1630–900 cm^{-1} is representative band assigned to cellulose. The additional peaks are seen in Fig. 2 (I-b) at 3000–2800 cm^{-1} , 1457 cm^{-1} , and 1376 cm^{-1} were contributed by –CH stretching and –CH₂ and –CH₃ bending vibrations of polypropylene (PP) molecules present in the TB paper (Kwiatkowski et al. 2016). The IR bands at 2995 and 2945 cm^{-1} are ascribed to the –CH stretching of PLA material (Fig. 2 (I-c)). The peaks at 1748 cm^{-1} , 1382 cm^{-1} and 1359 cm^{-1} seen in PLA material is characteristic of C=O stretching and CH bending, respectively. The peak due to the C–O–C group of PLA is present at 1180 cm^{-1} (Kwiatkowski et al. 2016). The FTIR spectrum of nylon tea bag paper is shown in Fig. 2 (I-d). The absorption peak at 3300 cm^{-1} , 2932 cm^{-1} and 2854 cm^{-1} , 1640 cm^{-1} and 1540 cm^{-1} are due to the N–H stretching, –CH₂–stretching, C=O stretching and N–H deformation and C–N stretching, respectively (El-Newehy et al. 2011).

Thermo gravimetric analysis

The thermal stability of the cellulosic, PLA and nylon papers was determined using TGA. The onset temperature denotes the beginning of weight loss while the final

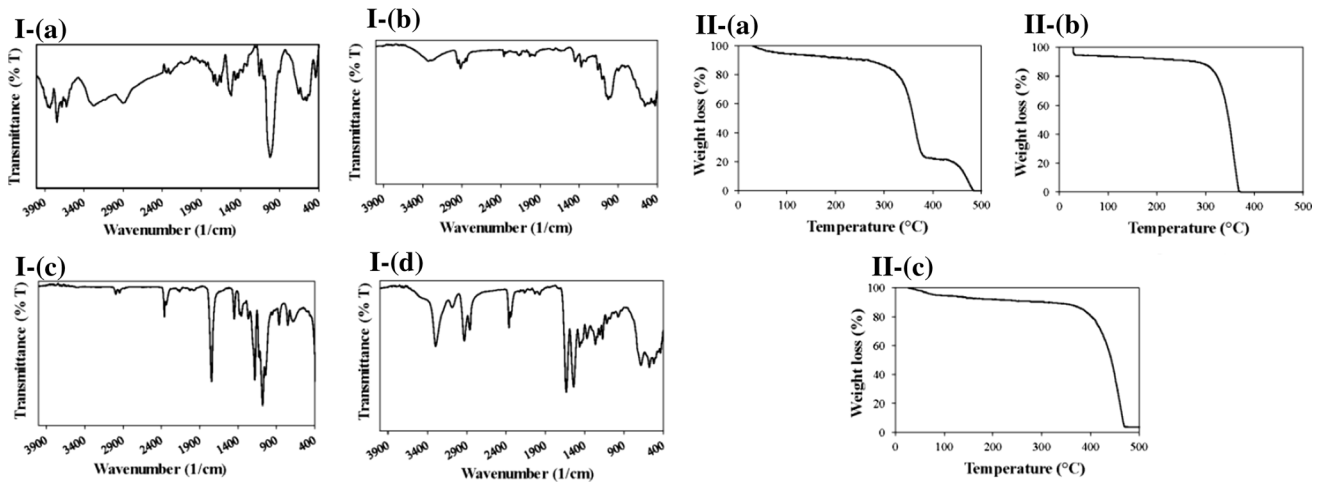


Fig. 2 (I) ATR-FTIR spectra of tea bag papers: **a** 100% cellulose (TB1), **b** cellulose/PP (TB2), **c** PLA (TB3) and **d** nylon (TB4). (II) TGA curves: **a** TB2, **b** TB3 and **c** TB4

temperature marks the completion of degradation. The cellulose/PP paper showed two degradation steps (Fig. 2 (II-a)). The weight loss around 250–300 °C is ascribed to the degradation of cellulose. (Yeng et al. 2015), while the distinct change around 440 °C is related to the degradation of PP (Mofokeng et al. 2012). This observation is in the corroboration of the IR spectra of the cellulose/PP paper. It can be perceived from Fig. 2 (II-b) that the PLA decomposition begins around 338.5 °C and completed at 388.9 °C, which supports the previously reported data (Mofokeng et al. 2012). The onset degradation temperature of the nylon paper is found to be 400 °C (Fig. 2 (II-c)), which is in accordance with that reported (El-Newehy et al. 2011).

Thickness and grammage of tea bag papers

The detail of thickness and grammage of tea bag papers are summarized in Table 1. Nylon paper thickness is comparable to the cellulosic papers but differs significantly in terms of grammage. Grammage of woven nylon paper is mean ~ 58%, ~ 30.5%, ~ 26% and 3% higher than cellulose, cellulose/PP, nylon hybrid and PLA tea bag paper, respectively. Thus, it can be inferred that individual fiber of nylon is heavier than other tea bag papers.

Wettability of tea bag papers

The contact angle is an indication of the wettability of a solid by a liquid. Contact angles lesser than 90° correspond to high wettability, while contact angles higher than 90° indicate low wettability. The advancing and receding contact angle of all tea bag papers are presented in Table 1. It can be perceived that the receding contact angle of all papers is lower than their respective advancing contact

angle. The receding contact angle is low presumably because the water 'wets out' the paper surface. It can also be interpreted from Eq. (1) that less the receding contact angle, more the net force required for withdrawing tea bag paper outside water. The lower receding contact angle may be due to the increase in weight of tea bag paper, after absorbing water when immersed (Son and Gardner 2007). The advancing contact angle of 100% cellulose paper (TB1) was lowest among all other papers indicating the hydrophilic nature of cellulose. Large amounts of hydroxyl groups are responsible for the hydrophilic properties of the cellulosic papers. All other tea bag papers (TB2, TB3, TB4, and TB5) showed an advancing contact angle higher than 80°. All these inferences indicate that these papers are relatively hydrophobic than 100% cellulose paper. The large contact angle is also a result of higher surface porosity and surface roughness (Oldani and Schock 1989). The advancing contact angle of 87.40° of cellulose/PP (TB2) also suggests the presence of PP, which renders the hydrophobicity to the tea bag paper.

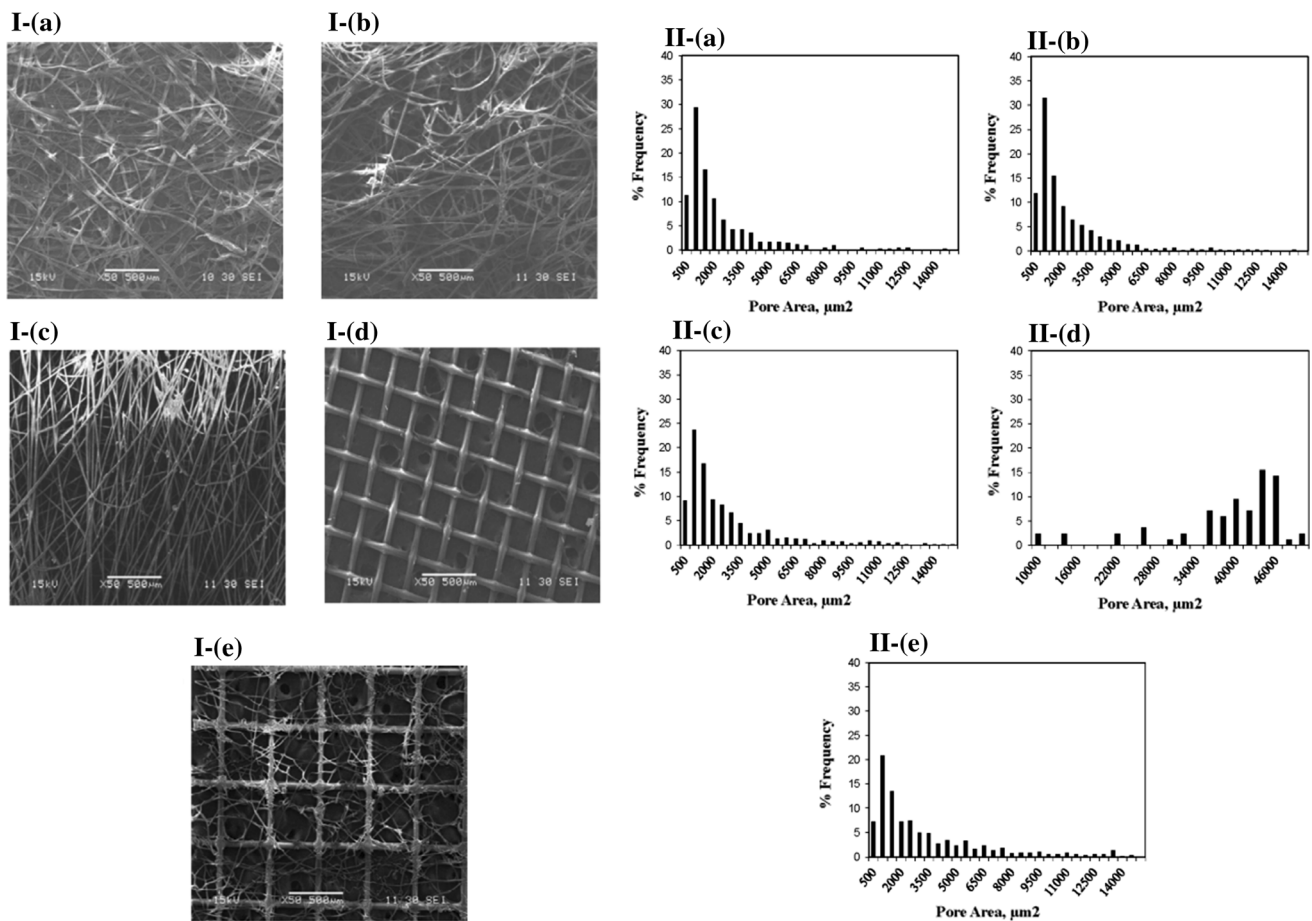
SEM image analysis

Pore area distribution and average pore size in tea bag papers

The SEM images of different tea bag papers were used to determine pore area determination. Figure 3 (I) depicts the SEM images of five different materials of tea bag papers. SEM images reveal that tea bag paper of cellulosic materials (TB1—Fig. 3 (I-a), TB2—Fig. 3 (I-b)) has irregular fiber morphology with a dense, compact and random arrangement of fibers. The cellulosic fibers are pleated randomly, creating irregular pores. The study unraveled that the fibers of TB3, i.e. PLA tea bag paper (Fig. 3 (I-c))

Table 1 Detailed specifications of tea bag papers

S. no.	Paper code	Grammage (g/m ²)	Thickness l_M (μm)	Advancing contact angle mean (ACA, °)	Receding contact angle mean (RCA, °)	Material
1	TB1	13.23	65 ± 1.61	50.49 ± 2.6	39.22 ± 2.2	100% cellulose
2	TB2	16.00	70 ± 2.10	87.40 ± 2.6	40.07 ± 4	Cellulose/PP
3	TB3	20.23	129 ± 1.31	84.90 ± 2.6	47.52 ± 1.1	PLA
4	TB4	20.89	75 ± 1.71	91.50 ± 1.2	9.36 ± 3.0	Nylon (woven)
5	TB5	16.56	73 ± 1.98	88.70 ± 0.8	6.3 ± 10.9	Nylon (hybrid)

**Fig. 3** (I) SEM images of representative tea bag papers **a** 100% cellulose (TB1), **b** cellulose/PP (TB2), **c** PLA (TB3), **d** woven nylon (TB4) and **e** nylon hybrid (TB5). (II) Pore area distribution: **a** TB1, **b** TB2, **c** TB3, **d** TB4 and **e** TB5

are comparatively smooth and ordered than that of cellulosic paper. SEM images of woven nylon tea bag paper (TB4—Fig. 3 (I-d)) showed a well patterned woven structure. Also, the pores present in woven nylon tea bag paper are found to be uniform and consistent when compared with other tea bag papers. Figure 3 (I-e) depicts the SEM image of a hybrid nylon paper (TB5). Both woven and non-woven nylon fibers are present in the case of

hybrid nylon paper. It is observed from the Fig. 3 (I-e) that nylon fibers are randomly arranged over the woven nylon fibers. Due to the random arrangement of nylon fibers, the pores are irregular and inconsistent throughout the tea bag paper.

Figure 3 (II) represents the pore area distribution for five different materials of tea bag papers. The cellulosic (TB1 and TB2), PLA (TB3) and nylon hybrid (TB5) tea bag

papers show major pore area distribution in the range of 1000–2000 μm^2 . The % frequency of pore area in the range of 1000–2000 μm^2 was found to be mean $\sim 20\%$ for cellulosic (TB1 and TB2), PLA (TB3) and nylon hybrid (TB5) papers. The distribution shifts to a larger pore area ($> 40,000 \mu\text{m}^2$) in the case of nylon tea bag paper which approximately accounts for 11.65% of the total pore area distribution (TB4—Fig. 3 (II-d)). The average pore area of tea bag paper is determined using pore area distribution data. The pore area distribution in tea bag paper with the highest % frequency contributes more to the average pore area of that tea bag paper.

The average pore area calculated for various tea bag papers was used for average pore size determination. The average size of the pores of cellulosic fibers is calculated to be 50 μm . It can also be seen that the fibers of TB3, i.e. PLA tea bag paper (Fig. 3 (I-c)) are comparatively smooth and ordered than that of cellulosic paper with an average pore size of 52 μm . The average pore size of PLA paper was found to be similar to that of cellulosic paper. Image analysis of woven nylon tea bag paper determined its average pore size (176.63 μm), which is approximately 3.7, 3.3, 3.4 and 2.7 times higher than that of 100% cellulose, cellulose/PP, PLA and nylon hybrid papers. Thus, the arrangement of fibers in the papers affects the average pore size. The uniform and patterned fibers lead to higher average pore size.

Porosity of tea bag papers

As presented in the Table 2, the %porosity of tea bag papers significantly depends upon the fibers orientation rather than the pore size. In the case of cellulosic tea bag papers (TB1 and TB2), the %porosity ranges from 20 to 30%. Though the average pore size of PLA paper (TB3) was found to be similar to that of the cellulosic paper, it differs greatly in terms of %porosity. The %porosity of PLA paper is at a higher range (38.49%) compared to that of cellulosic paper. This could be attributed to the relatively ordered orientation of PLA fibers than cellulosic fibers. In the nylon tea bag paper (TB4 and TB5) of different fiber orientations, woven and hybrid, the %porosity

is 62% and 46.79%, respectively. The order of porosity for these tea bag papers is seen as woven nylon > nylon hybrid > PLA > Cellulosic papers. Thus, it can be seen that the tea bag papers with uniform pore structures tend to have higher porosity than those with non-uniform pore structure. This lower porosity can be attributed to the random and inconsistent arrangement of fibers in cellulosic and PLA tea bag papers. The effect of these pore sizes, pore structure and porosity, can be seen on the permeance and infusion of tea components (GAE) through the tea bag papers.

Effect of pore structure and porosity on permeance of tea components through TB paper

To determine the effect of porosity of tea bag paper on infusion kinetics of tea, the permeance of tea solutes through different material of tea bag papers was determined. For the calculation of permeance of solutes through tea bag paper, $\ln(C_0/(2C_1 - C_0))$ was plotted against t , as per Eq. (12). Figure 4a shows the concentration versus time plot of PLA tea bag paper (TB3). As seen from the Fig. 4a, the experimental values showed a good linear fit for the PLA tea bag paper ($R^2 = 0.97$). The slope of the fitted line is equated to $\bar{P}A/V$ and permeance (\bar{P}) of PLA paper was calculated. Similar calculations were carried out for different tea bag papers of different materials. From different values of a slope, the permeance for different tea bag papers was calculated and correlated with %porosity values.

The %porosity and permeance values of different tea bags papers are summarized in Table. 2. It can be observed from the table that woven nylon (TB4) tea bag paper showed the highest permeance of 23.9×10^{-5} m/s. It was followed by nylon hybrid (TB5), PLA (TB3), cellulose/PP (TB2) and cellulose (TB1) with permeance values of 8.81×10^{-5} m/s, 5.87×10^{-5} m/s, 4.38×10^{-5} m/s and 2.43×10^{-5} , respectively.

The smaller permeance values of cellulosic papers can be attributed to the irregular pore structure, smaller pore size and low porosity of the paper. The pore structure plays an essential role in the permeance of tea solutes through tea

Table 2 Permeance and Initial rate data of different tea bag papers

Tea bag paper code	Average void size, D (m) $\times 10^5$	Porosity, ϵ (%)	Permeance (m/s) $\times 10^5$	k_i (mg/ml s) $\times 10^2$	Material
TB1	4.69	28.27	2.43	0.98	100% cellulose
TB2	5.32	32.56	4.38	1.05	Cellulose/PP
TB3	5.22	38.49	5.87	1.2	PLA
TB4	17.66	62	23.9	1.36	Nylon (woven)
TB5	6.46	46.79	8.81	1.3	Nylon (hybrid)

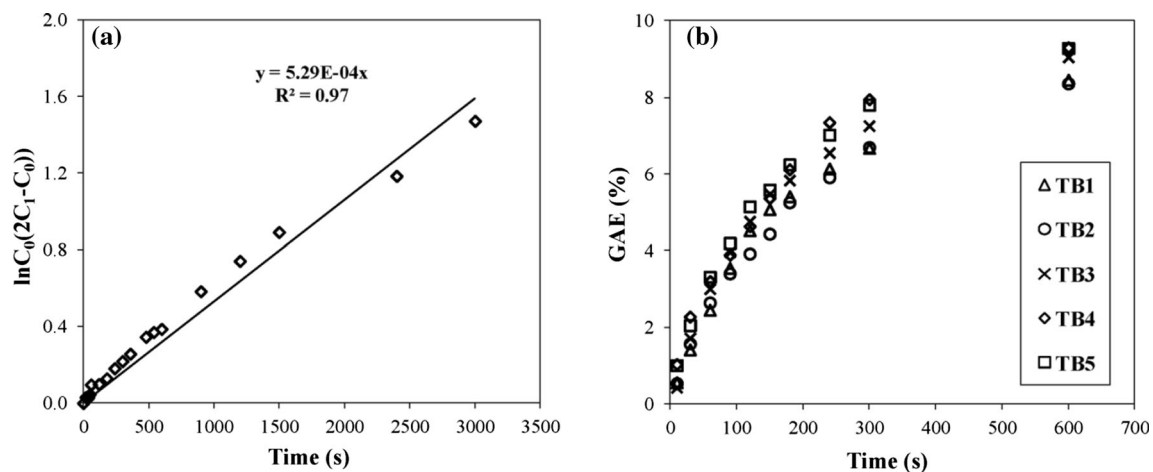


Fig. 4 **a** Representative plot of $\ln(C_0/(2C_1 - C_0))$ versus time for PLA (TB3), **b** infusion profiles of different TB papers

bag papers. It is perceived that the average pore size of PLA and cellulosic tea bag paper is similar (50μ). However, the permeance of PLA paper is found to be higher than that of cellulosic tea bag papers. This inference can be attributed to the effect of pore structure on the permeance of tea bag paper. As seen from the SEM images, the pore structure of the PLA is comparatively smooth and uniform than the cellulosic materials.

Similarly, the uniform pore structure and larger pore size eventually lead to higher porosity of woven nylon paper. This higher porosity resulted in the highest permeance of tea components through it. The permeance of woven nylon paper (TB4) is approximately 4 and 3 times higher than that of PLA and nylon hybrid paper, respectively. Though the material of TB4 and TB5 tea bag paper is 100% nylon, the presence of a random arrangement of fibers over woven paper led to non-uniform pore structures. Because of these inconsistently arranged fibers, the permeance of tea solutes is approximately three times lower than the woven nylon paper.

An increase in permeance was observed with an increase in %porosity for different tea bag papers (Table 2). When %porosity was plotted against permeance, a linear correlation was obtained. This correlation can be attributed to the permeance being strongly dependent on pore size and pore structure through which the tea solutes in infusion diffuses through a tea bag. The flow direction of diffusing solutes depends mainly on the pore structure rather than the overall porosity. The pore structure also determines the effective porosity, which primarily contributes to the permeance of tea solutes through tea bag paper (Ma and Morrow 1996). Also, the extent of wettability and swelling of tea bag papers may account for the permeance of tea components. Thus, these parameters should be taken into consideration for a better correlation between porosity with permeance.

Effect of tea bag permeance on infusion kinetics

Infusion profiles of tea in different tea bag papers in double chambered tea bags are illustrated in Fig. 4b. As seen in Fig. 4b, the initial rate of infusion of woven nylon tea bag paper is faster than other tea bag papers. In the case woven nylon paper, the GAE is approximately $\sim 30\%$, $\sim 21\%$ and $\sim 6.5\%$ higher than 100% cellulose, cellulose/PP, and PLA, respectively, at 1 min of infusion time. The GAE of woven nylon paper (TB4) is found to be approximately $\sim 10\%$, $\sim 11\%$, and $\sim 2.8\%$ higher than 100% cellulose, cellulose/PP and PLA, respectively at 10 min of infusion time. These inferences indicate that over time, the difference in the infusion rate diminishes. The GAE% of nylon hybrid at 1 and 10 min was found to be similar to that of woven nylon.

In the case of tea bag infusion, the initial infusion rate is critical as most of the consumers have a habit of dipping the tea bag for not more than 1 min. Thus, the initial rate of all tea bag papers was calculated and compared with their respective permeance value. The calculated k_i values of tea bags are summarized in Table 2. The data showed a good linear fit for all the studied tea bags. The R^2 obtained was always more than 0.90 for all tea bags. From Table 2, it can be observed that the initial infusion rate of woven nylon paper (TB4) is slightly faster than that of other tea bag papers. This is 1.2 times faster than all other tea bag papers on average. However, the permeance of these tea bag papers differs significantly. The permeance of woven nylon (TB4) is average ~ 10 , ~ 5.5 , ~ 4 and ~ 2.7 times higher than that of cellulose, cellulose/PP, PLA and nylon hybrid paper, respectively. The scale of difference in permeance values is 10 times, while the extent of difference in initial rate (k_i) is merely 1.38 times in the case of 100% cellulose paper. These inferences indicate that the

resistance offered by tea bag paper to the infusion is minimal. The major parameters affecting tea bag infusion kinetics are tea bed formed inside the tea bag, tea bag shapes and size, particle size of tea granules, tea bag loading, brewing temperature and dipping frequency (Yadav et al. 2017). In the present work, all these parameters were kept constant to observe the effect of permeance on tea infusion kinetics. It is observed that the tea bag paper has a negligible impact on tea infusion kinetics, despite having significantly different permeance values. Thus, it can be concluded that the permeance of tea solutes through tea bag does not have a significant impact on its infusion kinetics. This is in agreement with the findings reported by Spiro and Jaganyi (2000) for caffeine transport across a tea bag membrane. Their results suggested that the resistance to transfer caffeine across the porous tea bag membrane was negligible when compared with the filter paper of pore size 8 μ . These comparisons illustrate the significance of larger pore size, porosity and permeance of tea bag paper on tea bag infusion. The tea bag papers having high pore size and higher porosity shows the negligible resistance to the transport of tea solutes through the tea bag papers.

Conclusion

The tea bag paper parameters were successfully quantified in terms of pore area distribution, pore size, %porosity and permeance. The woven structure of nylon tea bag paper showed a larger pore size and %porosity. The influence of %porosity and pore size on permeance of different tea bag papers was investigated. With an increase in porosity, the permeance of tea components through the tea bag paper increases. The permeance of woven nylon tea bag paper was found to be the highest compared to that of non-woven (cellulosic, PLA and nylon hybrid) papers. This is due to the higher %porosity and uniform pore structure of woven nylon tea bag paper. Although the permeance of different tea bag papers is significantly different, their infusion profiles are approximately similar. This can be observed only when the resistance offered by tea bag paper is negligible to the transport of tea components. Permeance is a tea bag paper specific property which depends upon the pore structure and porosity. Infusion kinetics in porous tea bag paper is predominantly determined by diffusion within the tea leaves, permeability of tea bed inside the tea bag plus stirring outside the tea bag.

Acknowledgements One of the authors Pallavee P. Dhekne would like to thank the Pidilite Industries Ltd. for providing financial support.

References

- Astill C, Birch MR, Dacombe C, Humphrey PG, Martin PT (2001) Factors affecting the caffeine and polyphenol contents of black and green tea infusions. *J Agric Food Chem* 49:5340–5347. <https://doi.org/10.1021/jf010759+>
- Dhekne PP, Patwardhan AW (2020) Mathematical modeling of tea bag infusion kinetics. *J Food Eng* 274:109847. <https://doi.org/10.1016/j.jfoodeng.2019.109847>
- El-newehy MH, Al-deyab SS, Kenawy E, Abdel-megeed A (2011) Nanospider technology for the production of nylon-6 nanofibers for biomedical applications. *J Nanomater*. <https://doi.org/10.1155/2011/626589>
- Farakte RA, Yadav G, Joshi B, Patwardhan AW, Singh G (2016) Role of particle size in tea infusion process. *Int J Food Eng* 12:1–16. <https://doi.org/10.1515/ijfe-2015-0213>
- Harbowy ME, Balentine DA (1997) Tea chemistry. *Crit Rev Plant Sci* 16(5):415–480. <https://doi.org/10.1080/07352689709701956>
- Jaganyi D, Mdletshe S (2000) Kinetics of tea infusion. Part 2: the effect of tea-bag material on the rate and temperature dependence of caffeine extraction from black Assam tea. *Food Chem* 70:163–165. [https://doi.org/10.1016/S0308-8146\(99\)00262-9](https://doi.org/10.1016/S0308-8146(99)00262-9)
- Jaganyi D, Ndlovu T (2001) Kinetics of tea infusion. Part 3: the effect of tea bag size and shape on the rate of caffeine extraction from Ceylon orange pekoe tea. *Food Chem* 75:63–66. [https://doi.org/10.1016/S0308-8146\(01\)00186-8](https://doi.org/10.1016/S0308-8146(01)00186-8)
- Joshi BS, Farakte RA, Yadav GU, Patwardhan AW, Singh G (2016) Swelling kinetics of tea in hot water. *J Food Sci Technol* 53:315–325. <https://doi.org/10.1007/s13197-015-2023-9>
- Kwiatkowski P, Giedrys-kalemba S, Mizielińska M, Bartkowiak A (2016) Modification of PLA foil surface by ethylcellulose and essential oils. *J Microbiol Biotechnol Food Sci* 07:440–444. <https://doi.org/10.15414/jmbfs.2016.5.5.440-444>
- Ma S, Morrow NR (1996) Relationships between porosity and permeability for porous rocks. In: International symposium of the society of core analysts, pp 8–10
- Mofokeng JP, Luyt AS, Tábi T, Kovács J (2012) Comparison of injection moulded, natural fibre-reinforced composites with PP and PLA as matrices. *J Thermoplast Compos Mater* 25:927–948. <https://doi.org/10.1177/0892705711423291>
- Oldani M, Schock G (1989) Characterization of ultrafiltration membranes by infrared spectroscopy, ESCA, and contact angle measurements. *J Membr Sci* 43:243–258. [https://doi.org/10.1016/S0376-7388\(00\)85101-7](https://doi.org/10.1016/S0376-7388(00)85101-7)
- Price WE, Spiro M (1985) Kinetics and equilibria of tea infusion: theaflavin and caffeine concentrations and partition constants in several whole teas and sieved fractions. *J Sci Food Agric* 36:1303–1308. <https://doi.org/10.1002/jsfa.2740361215>
- Price WE, Spitzer JC (1993) The temperature dependence of the rate of extraction of soluble constituents of black tea. *Food Chem* 46:133–136
- Son J, Gardner DJ (2007) Dimensional stability measurements of thin wood veneers using the Wilhelmy plate technique. *Wood Fiber Sci* 36(1):98–106
- Spiro M, Jaganyi D (2000) Kinetics and equilibria of tea infusion, Part 15. Transport of caffeine across a teabag membrane in a modified rotating diffusion cell. *Food Chem* 69:119–124. [https://doi.org/10.1016/S0308-8146\(99\)00251-4](https://doi.org/10.1016/S0308-8146(99)00251-4)
- Spiro M, Jaganyi D, Broom MC (1992) Kinetics and equilibria of tea infusion: Part 9. The rates and temperature coefficients of caffeine extraction from green Chun Mee and black Assam Bukial teas. *Food Chem* 45:333–335. [https://doi.org/10.1016/0308-8146\(92\)90033-X](https://doi.org/10.1016/0308-8146(92)90033-X)
- Suteerapataranon S, Butsoongnern J, Punturat P, Jorpalit W, Thanomsilp C (2009) Caffeine in Chiang Rai tea infusions:

- effects of tea variety, type, leaf form, and infusion conditions. *Food Chem* 114:1335–1338. <https://doi.org/10.1016/j.foodchem.2008.11.013>
- UK Tea & Infusions Association (2010) The history of the tea bag. UK Tea & Infusions Association, London
- Yadav GU, Joshi BS, Patwardhan AW, Singh G (2017) Swelling and infusion of tea in tea bags. *J Food Sci Technol* 54:2474–2484. <https://doi.org/10.1007/s13197-017-2690-9>
- Yeng LC, Wahit MU, Othman N (2015) Thermal and flexural properties of regenerated cellulose (RC)/poly(3-hydroxybutyrate) (PHB) biocomposites. *J Teknol* 75:107–112. <https://doi.org/10.11113/jt.v75.5338>
- Yuan Y, Lee TR (2013) Contact angle and wetting properties. In: Bracco G, Holst B (eds) *Surface science techniques*. Springer, Berlin, pp 3–34

Publisher's Note Springer Nature remains neutral with regard to jurisdictional claims in published maps and institutional affiliations.